Acta Pharmacologica Sinica (2017) 38: 69–79
 1671-4083/17
www.nature.com/aps

Original Article

Alisol B 23-acetate protects against non-alcoholic steatohepatitis in mice via farnesoid X receptor activation

Qiang MENG[1, 2, *], Xing-ping DUAN[1], Chang-yuan WANG[1, 2], Zhi-hao LIU[1, 2], Peng-yuan SUN[1, 2], Xiao-kui HUO[1], Hui-jun SUN[1, 2], Jin-yong PENG[1], Ke-xin LIU[1, 2, *]

[1]Department of Clinical Pharmacology, College of Pharmacy, Dalian Medical University, Dalian 116044, China; [2]Key Laboratory of Pharmacokinetics and Transport of Liaoning Province, Dalian Medical University, Dalian 116044, China

Abstract

Alisol B 23-acetate (AB23A) is a natural triterpenoid isolated from the traditional Chinese medicine rhizoma alismatis, which exhibits a number of pharmacological activities, including anti-hepatitis virus, anti-cancer and antibacterial effects. In this study we examined whether AB23A protected against non-alcoholic steatohepatitis (NASH) in mice, and the mechanisms underlying the protective effects. NASH was induced in mice fed a methionine and choline-deficient (MCD) diet for 4 weeks. The mice were simultaneously treated with AB23A (15, 30, and 60 mg·kg^{-1}·d^{-1}, ig) for 4 weeks. On the last day, blood samples and livers were collected. Serum liver functional enzymes, inflammatoru markers were assessed. The livers were histologically examined using H&E, Oil Red O, Masson's trichrome and Sirius Red staining. Mouse primary hepatocytes were used for *in vitro* experiments. The mechanisms underlying AB23A protection were analyzed using siRNA, qRT-PCR, and Western blot assays. AB23A treatment significantly and dose-dependently decreased the elevated levels of serum ALT and AST in MCD diet-fed mice. Furthermore, AB23A treatment significantly reduced hepatic triglyceride accumulation, inflammatory cell infiltration and hepatic fibrosis in the mice. AB23A-induced decreases in serum and hepatic lipids were related to decreased hepatic lipogenesis through decreasing hepatic levels of SREBP-1c, FAS, ACC1 and SCD1 and increased lipid metabolism via inducing PPARα, CPT1α, ACADS and LPL. The reduction in inflammatory cell infiltration corresponded to deceased serum levels of mKC and MCP-1 and decreased hepatic gene expression of MCP-1 and VCAM-1. The reduction in hepatic fibrosis was correlated with decreased hepatic gene expression of fibrosis markers. The protective effects of AB23A were FXR-dependent, because treatment with the FXR agonist CDCA mimicked AB23A-induced hepato-protection in the mice, whereas co-administration of FXR antagonist guggulsterone abrogated AB23A-induced hepato-protection. In mouse primary hepatocytes, FXR gene silencing abrogated AB23A-induced changes in gene expression of Apo C-II, CPT1α, ACADS and LPL. AB23A produces protective effects against NASH in mice via FXR activation.

Keywords: hepatic inflammation; non-alcoholic steatohepatitis; hepatic fibrosis; alisol B 23-acetate; farnesoid X receptor; CDCA; guggulsterone

Acta Pharmacologica Sinica (2017) 38: 69–79; doi: 10.1038/aps.2016.119; published online Oct 24 2016

Introduction

Non-alcoholic fatty liver disease (NAFLD), whose hallmark is the accumulation of fat in the liver in the absence of alcohol consumption, is highly prevalent in Western countries[1, 2]. Non-alcoholic steatohepatitis (NASH), a subtype of NAFLD in which steatosis is accompanied by inflammation and hepatocyte damage, is increasingly being recognized as an important cause of liver-related morbidity and mortality[3, 4]. Currently, there is no proven effective therapy for NASH, and liver transplantation is the only option for end-stage NASH cirrhosis[5]. Therefore, there is an urgent medical need to develop drugs for the treatment of this disease.

The pathogenesis of NASH is multifactorial and only partially understood; however, lipid homeostasis plays a critical role in the disease process[6]. In NASH patients, liver fat (mainly triglycerides) is derived from free fatty acids that are obtained mainly from diet, *de novo* synthesis or adipose tissue. When triglyceride synthesis is increased and fatty acid metabolism is impaired in the liver, the capacity of the liver

*To whom correspondence should be addressed.
E-mail mengq531@163.com (Qiang MENG);
kexinliu@dlmedu.edu.cn (Ke-xin LIU)
Received 2016-07-05 Accepted 2016-08-26

to store triglycerides is overwhelmed, and NASH begins to develop[7]. Research on ligand-dependent nuclear receptors in recent decades has provided new opportunities to elucidate the pathogenesis of NASH and find effective treatments. The farnesoid X receptor (FXR; NR1H4), a member of the nuclear hormone receptor superfamily of ligand-activated transcription factors, is highly expressed in the liver, intestine, kidney and adrenal glands[8, 9]. FXR has been demonstrated to play a central role in the progression of NASH[10, 11]. FXR regulates genes that are involved in lipid and lipoprotein metabolism, including sterol regulatory element-binding protein 1c (SREBP-1c), apolipoprotein C-II (Apo C-II), and apolipoprotein C-III (Apo C-III)[12–15]. FXR has been demonstrated to be activated by physiological concentrations of bile acids or by exogenous FXR ligands[16, 17].

Currently, NASH treatments include dietary changes, exercise and drug treatments, such as metformin, statins and fibrates; however, these drugs have some adverse effects or contraindications. Therefore, new candidate drugs with high efficacy and few or no side effects are urgently needed for treating NASH. Traditional Chinese medicines are rich sources of biologically active substances that can be used to prevent human diseases. Alisol B 23-acetate (AB23A) is a natural triterpenoid isolated from Rhizoma alismatis, which is a medicinal plant that has been widely used as a traditional Chinese medicine for a long period of time[18]. Its chemical structure is shown in Figure 1A. In recent years, AB23A has been biologically characterized, and several pharmacological activities have been demonstrated, including anti-hepatitis virus activity, anti-proliferative activity in cancer cell lines and antibacterial effects[19–21]. AB23A has been shown to induce Bax nuclear translocation and apoptotic cell death in human hormone-resistant prostate cancer PC-3 cells and to have anti-proliferative, anti-migration and anti-invasion activities in ovarian cancer cells[22, 23]. Additionally, AB23A has also been shown to have some hepatoprotective effects[24]. Therefore, an important and intriguing question arises as to whether AB23A might have protective effects against NASH. We have recently demonstrated that AB23A promotes liver regeneration via FXR activation[25]. Thus, if AB23A indeed possesses protective effects against NASH, a further question is whether FXR and its target genes contribute to liver protection.

In the present study, we demonstrate that AB23A inhibits hepatic triglyceride accumulation and protects against hepatic inflammation and fibrosis in mice fed a methionine and choline-deficient (MCD) diet. We further explored the potential mechanisms of these protective effects *in vivo* and *in vitro*.

Materials and methods

Chemicals and reagents

AB23A (purity >98%) was purchased from Chengdu Must Bio-technology Co, Ltd (Chengdu, China). Chenodeoxycholic acid (CDCA, purity>98%) and guggulsterone (GS, purity >98%) were purchased from Sigma-Aldrich (St Louis, MO, USA). Alanine aminotransferase (ALT), aspartate aminotransferase (AST), triglycerides, free fatty acids, and total cholesterol detection kits were obtained from the Nanjing Jiancheng Institute of Biotechnology (Nanjing, China). Monocyte chemotactic protein 1 (MCP-1) and mouse keratinocyte-derived chemokine (mKC) detection kits were obtained from Meso Scale Diagnostics (Maryland, USA). Enhanced BCA Protein Assay Kits and Tissue Mitochondria Isolation Kits were provided by the Beyotime Institute of Biotechnology (Jiangsu, China). Tissue Protein Extraction Kits were purchased from KeyGEN Biotech Co, Ltd (Nanjing, China). Tris and sodium dodecyl sulfate (SDS) were purchased from Sigma-Aldrich (St Louis, MO, USA). RNAiso Plus, a PrimeScript® RT reagent kit with gDNA Eraser (Perfect Real Time) and SYBR® *Premix Ex Taq*™ II were purchased from TaKaRa Biotechnology Co, Ltd (Dalian, China). Rabbit anti-SREBP-1c, rabbit anti-fatty acid synthetase (FAS), rabbit anti-acetyl CoA carboxylase 1 (ACC1) and rabbit anti-stearoyl CoA desaturase 1 (SCD1) antibodies were purchased from Proteintech Group, Inc (Chicago, USA).

Animals and treatments

All animal maintenance and treatment protocols were in accordance with the Guide for the Care and Use of Laboratory Animals from the National Institutes of Health and were approved by the Institutional Animal Care and Use Committee at Dalian Medical University, Dalian, China. Male C57BL/6 mice (8–9 weeks) were housed in laboratory animal facilities under a 12-h light/dark cycle with access to standard chow and water *ad libitum*. C57BL/6 mice were divided into the following 7 experimental groups (n=8 per group) and fed and treated as follows for 4 weeks: (1) control group fed a control chow diet (A02082003B, Research Diets, New Brunswick, USA), (2)group fed a normal diet with a daily oral gavage of AB23A (60 mg/kg, AB23A60), (3) disease model group fed an MCD diet (A02082002B, Research Diets, New Brunswick, USA) with a daily oral gavage of vehicle (10% hydroxypropyl-beta-cyclodextrin in 500 mmol/L phosphate pH 7.0), (4) group fed an MCD diet with a daily oral gavage of low-dose AB23A (15 mg/kg, AB23A15), (5) group fed an MCD diet with a daily oral gavage of medium-dose AB23A (30 mg/kg, AB23A30), (6) group fed an MCD diet with a daily oral gavage of high-dose AB23A (60 mg/kg, AB23A60), and (7) group fed an MCD diet with a daily oral gavage of CDCA (60 mg/kg, CDCA60). We monitored food intake and found no differences among the experimental groups. On the last day, mice were orally administered with either vehicle or compound in the morning, fasted for 3.5 h, and then blood was collected by cardiac puncture and the livers were dissected and fixed in 10% formalin for histological analysis or snap frozen in lipid nitrogen for future analyses.

Biochemical analysis

Serum ALT, AST, MCP-1, mKC, triglycerides, free fatty acids, total cholesterol and hepatic triglycerides, free fatty acids, and total cholesterol were analyzed using commercial kits according to the manufacturers' protocols.

Histopathology

Liver fragments were fixed in 10% neutral buffered formalin, embedded in paraffin, sliced into 5 μm sections, stained with either H&E, Masson's trichrome or Sirius Red staining using standard protocols and then examined microscopically for structural changes. For Oil Red O staining, fresh liver tissues were embedded in optimum cutting temperature (OCT) compound and cryo-sectioned. The sections were fixed in 4% paraformaldehyde in PBS and were stained with 0.3% Oil Red O according to standard procedures. The Sirius Red stained sections (5 randomly selected fields/section at ×20 magnification) were quantified by using MetaVue imaging software (Molecular Devices, Downingtown, PA, USA).

Isolation and culture of mouse primary hepatocytes

Hepatocytes from male C57BL/6 mice (8–9 weeks) were isolated by the two-step collagenase digestion method as described previously[26]. The obtained hepatocytes were cultured with the William's E medium, supplemented with 0.1 μmol/L dexamethasone (Sigma-Aldrich, St Louis, MO, USA), 10% heat-inactivated fetal bovine serum, 100 U penicillin/streptomycin, 1×insulin-transferrin-selenium-sodium pyruvate solution (Gibco, NY, USA) and 1× glutamine on plates coated with collagen, and then incubated for 3 h. The William's E medium was then exchanged, and the cells were incubated for another 9 h to a density of 6×10^5 cells per well. The cells were treated with DMSO (0.1%) or AB23A (1, 5, 10 or 20 μmol/L) for 48 h.

RNA silencing experiment

Mouse primary cultured hepatocytes were seeded onto 12-well plates at a density of 6×10^5 cells per well. Twelve hours later, 200 nmol/L negative control siRNA or siRNA targeting mouse FXR (siGENOME SMARTpool, Dharmacon) was transiently transfected into mouse primary cultured hepatocytes by using Lipofectamine 2000™ (Invitrogen, Carlsbad, USA) and incubated for 60 h. Then, 10 μmol/L AB23A was added to the culture medium for 48 h. After that, the cells were harvested for quantitative real-time PCR analysis.

Quantitative real-time PCR

Total RNAs from mouse hepatic tissue or mouse primary hepatocytes were extracted with RNAiso Plus reagent according to the manufacturer's instructions. Total RNAs (1 μg) was reverse-transcribed to cDNA with a PrimeScript® RT reagent kit. The levels of mRNA expression were quantified using SYBR Green PCR Master Mix and an ABI Prism 7500 Sequence Detection System (Applied Biosystems, USA). The quantity of mRNA was normalized with mouse β-actin as an internal standard.

Protein isolation and Western blotting

Liver tissues were homogenized in protein lysis buffer containing 1 mmol/L PMSF. Fifty μg of total protein was resolved with 8%–12% SDS-PAGE and transferred onto PVDF membranes. After blocking with 5% non-fat dry milk in Tris-buffered saline, membranes were incubated overnight with primary antibodies. Specific bands were detected by an enhanced chemiluminescence (ECL) method using the Bio-Spectrum Gel Imaging System (UVP, USA).

Statistical analysis

Data are expressed as the mean±SD. Statistical analysis between two groups was performed with Student's *t*-tests, and multiple comparisons were performed with one-way ANOVAs. $P<0.05$ was considered statistically significant.

Results

Effects of AB23A on serum liver functional enzymes, serum inflammatory markers, and liver histopathology

Serum ALT and AST, which are biochemical indicators of hepatic cell damage and diagnostic markers for the presence of NASH, were both substantially increased by the MCD diet, and AB23A treatment significantly reduced these increases in serum ALT and AST in a dose-dependent manner (Figure 1B, 1C). CDCA, a known FXR agonist, was used as a positive control. To evaluate liver histological changes, liver sections were stained with H&E. Obvious hepatocyte ballooning and severe macrovesicular steatosis with marked inflammatory cell infiltration were observed in the livers of the MCD mice. AB23A treatment significantly reduced the degree of liver steatosis and inflammatory cell infiltration in mice (Figure 1D). Furthermore, the inflammatory markers serum MCP-1 and mKC were increased 3.4-fold and 2.3-fold, respectively, in the MCD mice and were both decreased by AB23A treatment in a dose-dependent manner, with a maximal decrease at a dose of 60 mg/kg (Figure 1E, 1F). Altogether, these results suggest that AB23A treatment results in a beneficial effect on hepatic function and inflammation.

Effects of AB23A on serum lipids and hepatic triglycerides

Because hepatic lipid deposition is a key component of NASH, the effects of AB23A treatment on serum and hepatic lipids were determined. The serum levels of triglycerides, free fatty acids and total cholesterol were higher in MCD mice than in control mice. After AB23A treatment, the concentrations of triglycerides, free fatty acids and total cholesterol were markedly decreased in a dose-dependent manner (Figure 2A–2C). Similarly to the serum results, AB23A reversed the increases in the hepatic levels of triglycerides, free fatty acids and total cholesterol induced by the MCD diet (Figure 2D–2F). Because the best hepatoprotective effects were found in the high-dose group, 60 mg/kg of AB23A was chosen for the follow-up study. The morphometric analysis of liver sections stained with Oil Red O, a measure of liver triglyceride accumulation, confirmed this observation. A significant decrease in neutral lipids was observed in mice treated with AB23A (Figure 2G). These results suggest that AB23A has substantial lipid-lowering effects in a mouse NASH model.

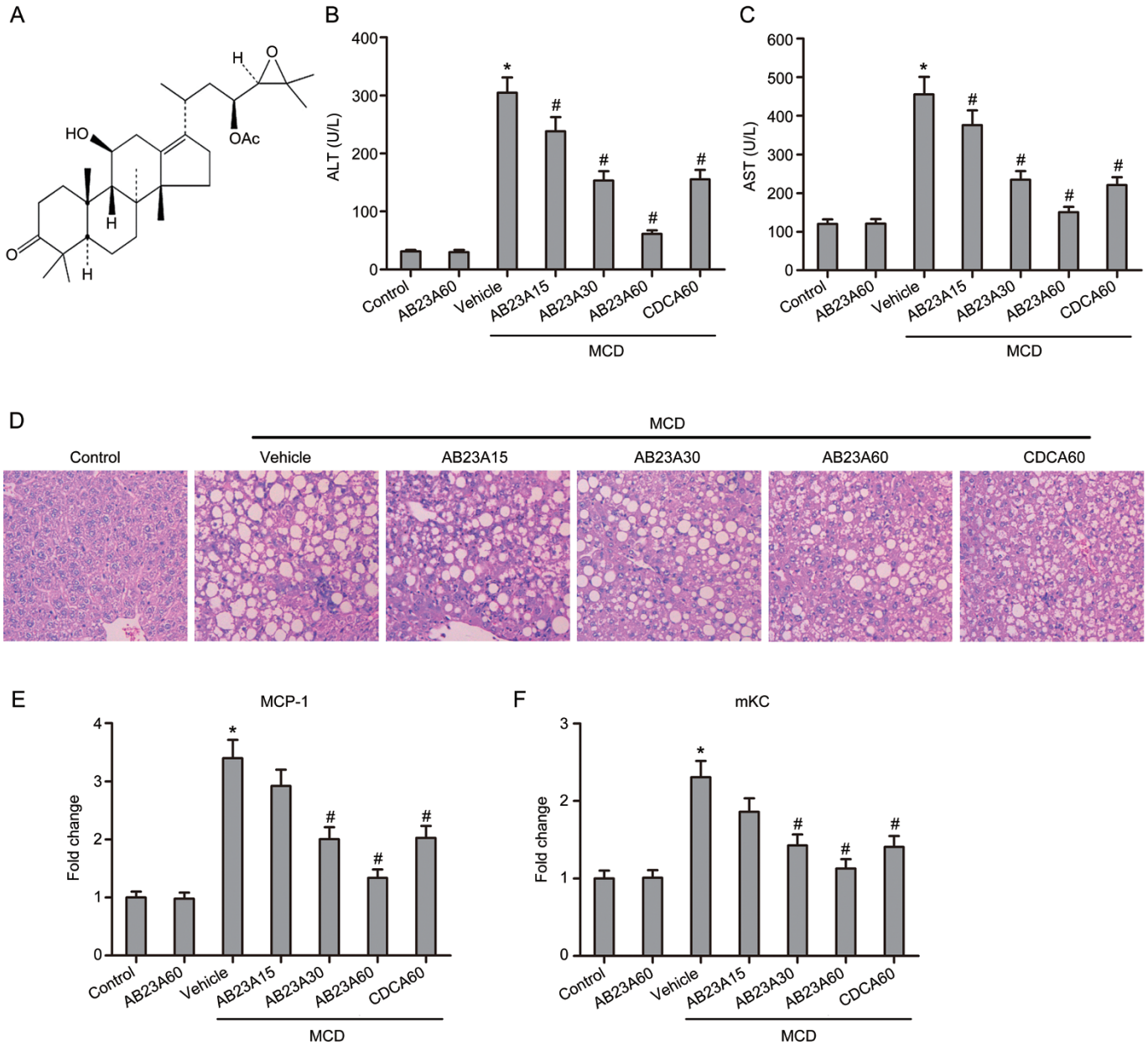

Figure 1. Effects of AB23A on serum liver enzymes, histopathology and serum inflammatory markers. (A) The chemical structure of AB23A. Serum ALT (B) and AST (C) levels elevated by MCD were significantly reduced by treatment with different doses of AB23A. Data are the mean±SD. n=8. $^{*}P$<0.05 *vs* control. $^{\#}P$<0.05 *vs* MCD+vehicle. AB23A attenuated liver injury induced by the MCD diet in mice. (D) Representative images of H&E stained liver sections (×400 magnification). Serum MCP-1 (E) and mKC (F) levels were reduced by AB23A in a dose-dependent manner. Data are the mean±SD. n=8. $^{*}P$<0.05 *vs* control. $^{\#}P$<0.05 *vs* MCD+vehicle.

Effects of AB23A on the hepatic expression of proteins involved in triglyceride and fatty acid synthesis

To clarify the mechanism underlying the decreased lipid levels in AB23A-treated mice, we determined the expression levels of proteins involved in lipogenesis in the mice. Hepatic lipogenesis is mainly modulated by SREBP-1c, which is a master regulator of lipid biosynthesis and regulates the expression of several genes involved in triglyceride and fatty acid synthesis, including FAS, ACC1 and SCD1. The hepatic protein expression levels of SREBP-1c, FAS, ACC1 and SCD1 were significantly increased in the MCD mice compared with the control mice. In contrast, decreases in SREBP-1c, FAS, ACC1 and SCD1 protein were observed in AB23A-treated MCD mice (Figure 3A). These results suggest that AB23A suppresses hepatic lipogenesis synthesis, thus resulting in decreases in plasma and liver lipid levels.

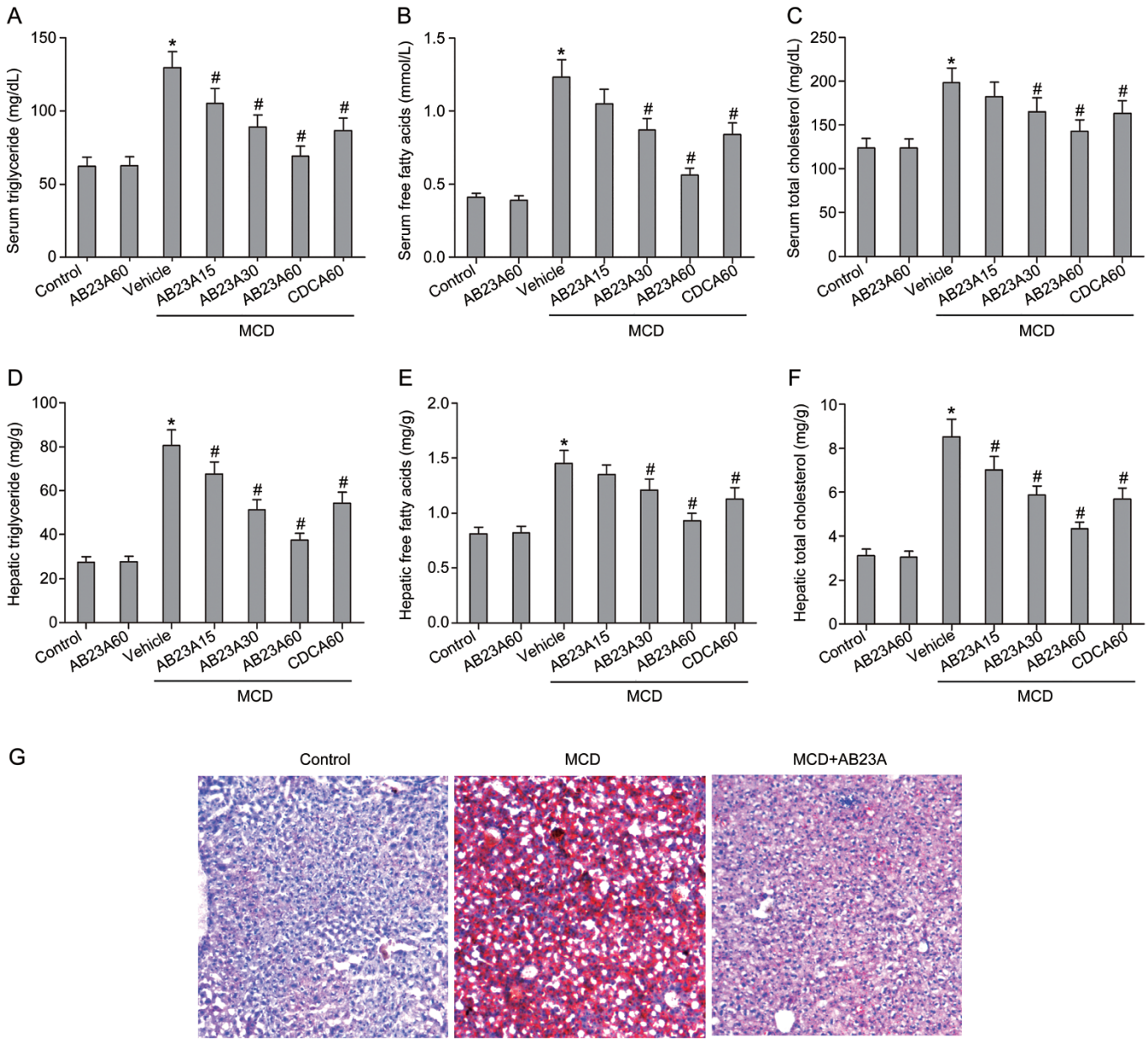

Figure 2. Effects of AB23A on serum and hepatic lipid triglyceride content. Serum levels of triglycerides (A), free fatty acids (B) and total cholesterol (C) were increased by the MCD diet and were reduced by AB23A treatment. Similarly to the serum results, AB23A reversed the increases in hepatic levels of triglycerides (D), free fatty acids (E) and total cholesterol (F) induced by the MCD diet. (G) Oil Red O staining of liver sections from control, MCD, and MCD+AB23A mice (400× magnification).

Effects of AB23A on the hepatic expression of genes involved in triglyceride and fatty acid metabolism

To further determine the mechanism underlying the decreased lipid levels in AB23A-treated mice, we first examined the hepatic expression of genes involved in fatty acid β-oxidation. The gene expression levels of carnitine palmitoyl transferase 1α (CPT1α) and acyl-coenzyme A dehydrogenase (ACADS), two key enzymes in the β-oxidation of fatty acids, were decreased by the MCD diet and were increased with AB23A treatment. Additionally, CPT1α and ACADS expression levels are modulated by peroxisome proliferator-activated receptor α (PPARα), a nuclear hormone receptor. PPARα mediates the esterification of fatty acids and increases lipoprotein metabolism. As shown in Figure 3B, AB23A treatment increased PPARα expression.

Furthermore, the lipolysis of triglyceride-rich lipoproteins is mainly mediated by lipoprotein lipase (LPL), whose activity is up-regulated by Apo C-II and down-regulated by Apo C-III and angiopoietin-like 3 (ANGPTL3). AB23A treatment induced Apo C-II and inhibited Apo C-III and ANGTPL3 expression, thus leading to LPL activation (Figure 3C). These results indicate that AB23A promotes triglyceride metabolism

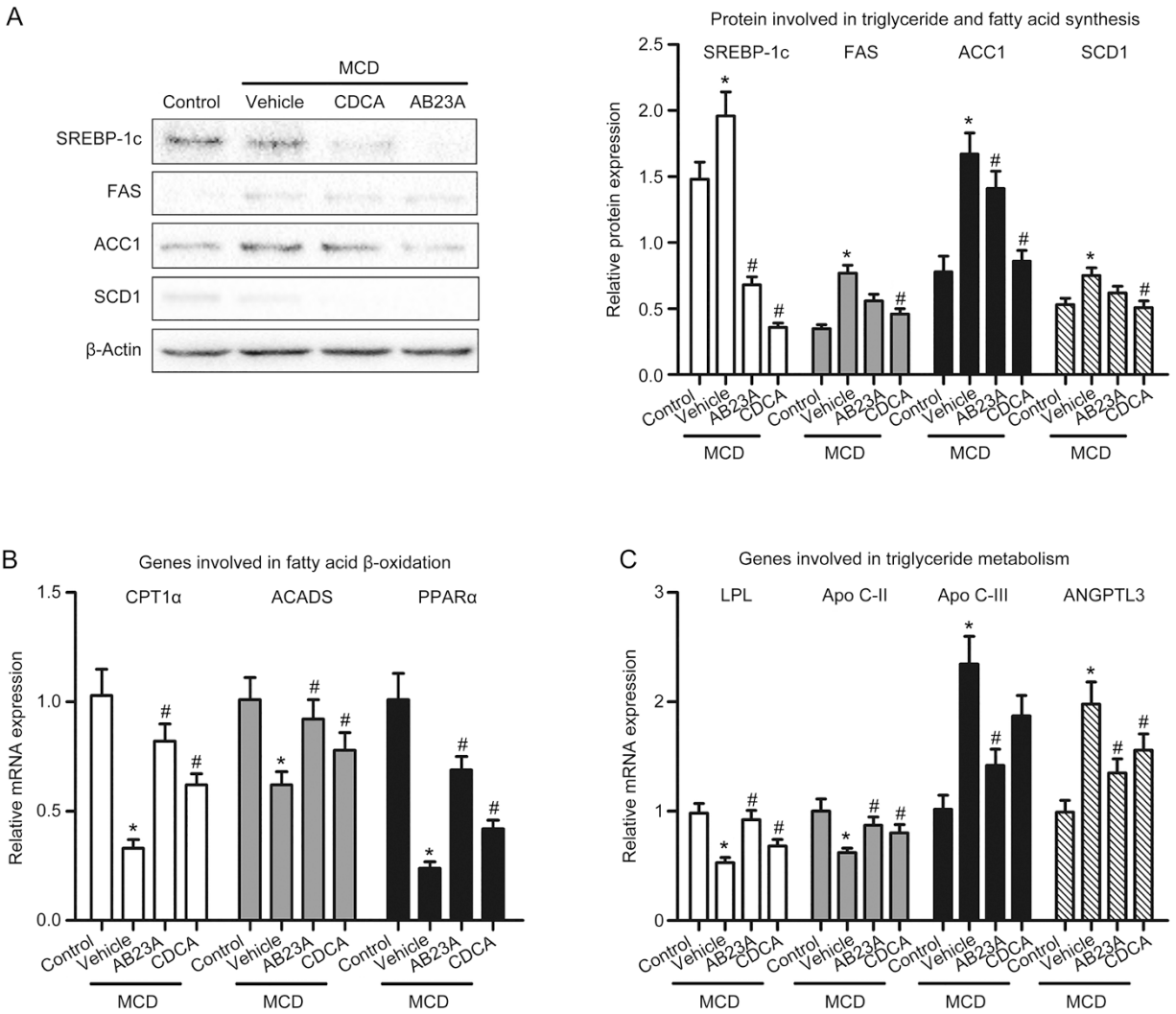

Figure 3. Effects of AB23A on the hepatic expression of proteins or genes involved in triglyceride and fatty acid synthesis and metabolism. (A) The expression of proteins involved in triglyceride and fatty acid synthesis, including SREBP-1c, FAS, ACC1 and SCD1 was increased by the MCD diet and was reduced by AB23A treatment. Data are the mean±SD. n=5. $^{*}P$<0.05 *vs* control. $^{\#}P$<0.05 *vs* MCD+vehicle. AB23A increased the gene expression of CPT1α, ACADS and PPARα, which are involved in fatty acid β-oxidation (B). AB23A also increased the lipolysis of triglyceride-rich lipoproteins through regulating the gene expression of Apo C-II, Apo C-III, ANGPTL3 and LPL (C). Data are the mean±SD. n=5. $^{*}P$<0.05 *vs* control. $^{\#}P$<0.05 *vs* MCD+vehicle.

by inducing LPL activity. Altogether, these results suggest that AB23A promotes triglyceride and fatty acid metabolism, thus resulting in decreases in serum and hepatic lipid levels.

Effects of AB23A on liver inflammation

Because AB23A treatment decreased the MCD diet-induced elevation of serum MCP-1 and mKC (Figure 1E, 1F), hepatic inflammatory gene expression was next examined. As shown in Figure 4A, MCP-1 and vascular cell adhesion molecule-1 (VCAM-1) mRNA levels were higher in the MCD mice compared with the control mice. AB23A treatment reversed these MCD diet-induced increases in inflammatory gene expression. These data indicate that AB23A treatment significantly reduces hepatic inflammation caused by the MCD diet.

Effects of AB23A on liver fibrosis

The MCD diet has previously been shown to cause marked hepatic fibrosis[27]. As shown in Figure 4B, 4C, the hepatic fibrosis genes a1(I) collagen, a2(I) collagen, α-smooth muscle actin (a-SMA), transforming growth factor-β1 (TGF-β1), matrix metalloprotein-2 (MMP-2) and tissue inhibitor of metalloproteinase-1 (TIMP-1) were increased by the MCD diet, thus suggesting significant hepatic stellate cell (HSC) activation and hepatic fibrosis caused by this diet. AB23A treatment significantly attenuated the induction of all of the fibrotic genes, thus resulting in marked protection against HSC activation and hepatic fibrosis. The beneficial effects of AB23A treatment on hepatic fibrosis were then further confirmed using Masson's Trichrome and Sirius Red staining of the liver sections. The

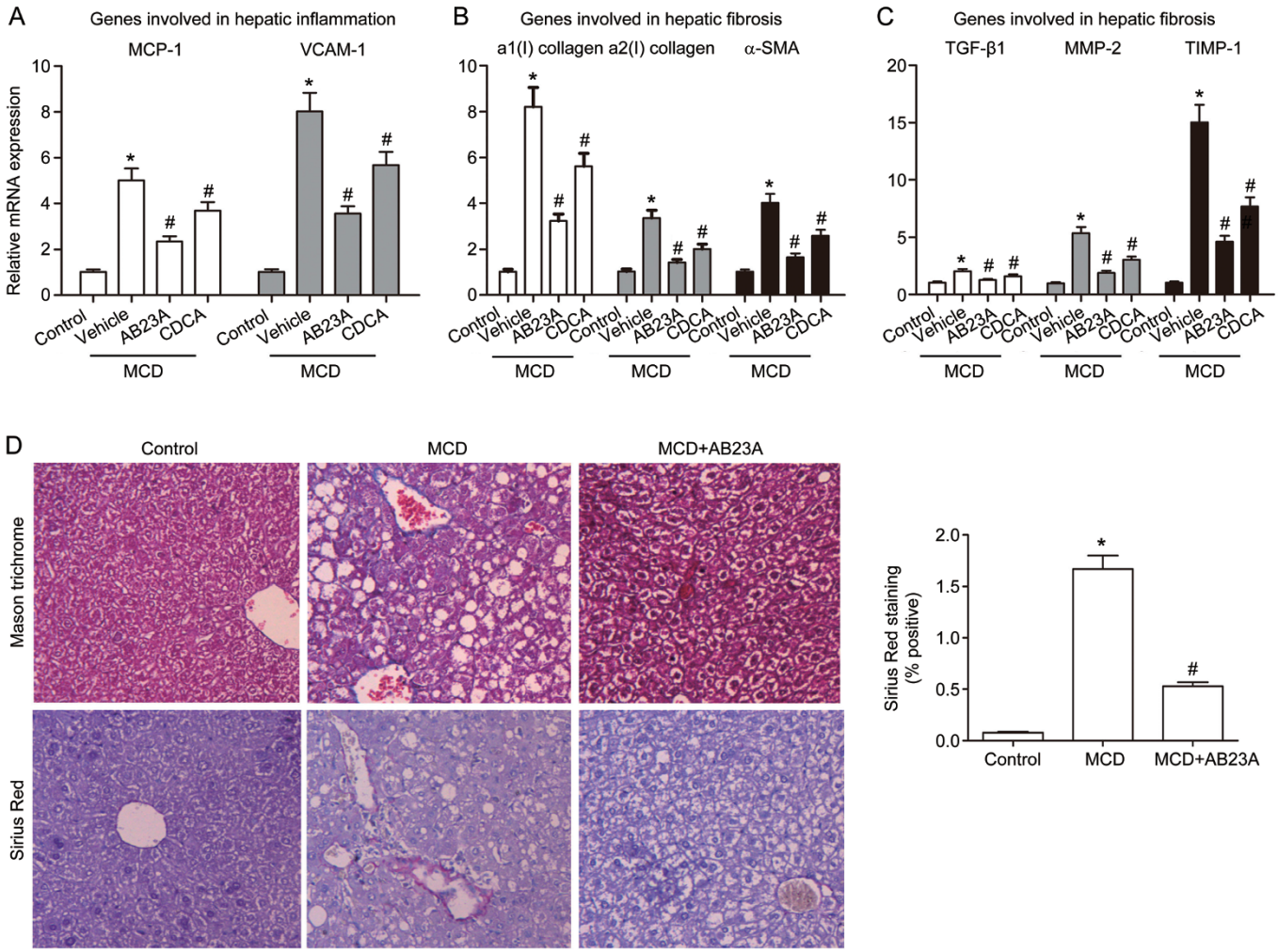

Figure 4. Effects of AB23A on liver inflammation and fibrosis. (A) Gene expression levels of MCP-1 and VCAM-1, both of which are hepatic inflammatory genes, were determined by quantitative RT-PCR analysis. (B) and (C) Hepatic fibrosis genes: a1(I) collagen, a2(I) collagen, α-SMA, TGF-β1, MMP-2 and TIMP-1, were increased by the MCD diet and were reduced by AB23A treatment. Data are the mean±SD. n=5. $^{*}P$<0.05 *vs* control. $^{\#}P$<0.05 *vs* MCD+vehicle. (D) Masson's Trichrome staining and Sirius Red staining of liver sections (400×magnification). Morphometric analysis of Sirius Red-stained sections. Data are the mean±SD. n=5. $^{*}P$<0.05 *vs* control. $^{\#}P$<0.05 *vs* MCD.

MCD diet caused extensive fibrosis at 4 weeks, as evidenced by the blue collagen staining using Masson's Trichrome stain and the red collagen staining using the Sirius Red stain (Figure 4D). AB23A treatment resulted in a robust reduction in collagen staining with both staining methods. Altogether, these results indicate that the beneficial effects of AB23A on the development of MCD diet-induced NASH results from limiting HSC activation and collagen deposition.

AB23A alters gene expression involved in hepato-protection and protects against MCD-induced NASH via FXR

Because SREBP-1c and the genes involved in triglyceride and fatty acid metabolism are downstream target genes of FXR and AB23A has been shown to promote liver regeneration via FXR activation[25], we hypothesized that AB23A might activate FXR and consequently protect against NASH in mice. To verify this hypothesis, we blocked FXR with the FXR antagonist GS in mice. Co-administration of the antagonist abrogated the decrease in SREBP-1c, FAS, ACC1 and SCD1 protein caused by AB23A (Figure 5A). GS also abrogated the increases in the expression of PPARα, CPT1α, ACADS and LPL induced by AB23A (Figure 5B). Furthermore, the protective effect of AB23A was reduced by GS administration (Figure 5C). Altogether, these results clearly demonstrate that AB23A protects against NASH by activating FXR *in vivo*.

The regulation of FXR target gene expression by AB23A is abrogated by FXR gene silencing *in vitro*

In the *in vivo* experiments, the effects of AB23A on the expression of FXR target genes have been measured; however, the changes may not be sufficient to represent the effects of AB23A on FXR activation. Thus, the effects of AB23A on FXR activation were subsequently examined using mouse primary cultured hepatocytes and FXR gene silencing experiments *in vitro*.

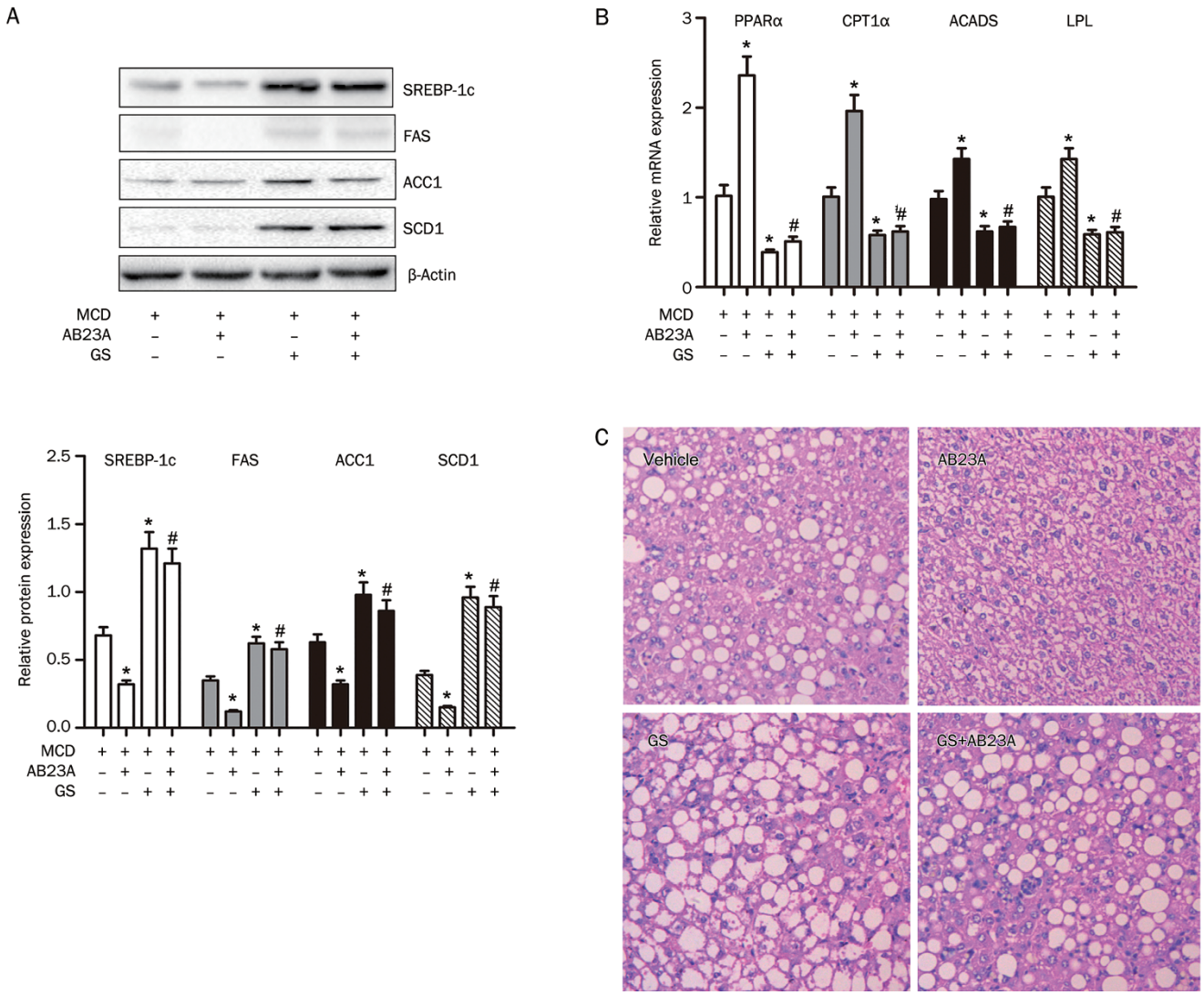

Figure 5. Effects of AB23A on the regulation of proteins and genes involved in lipid homeostasis are abrogated by the FXR antagonist GS. (A) The hepatic expression of SREBP-1c, FAS, ACC1 and SCD1 in mice treated with vehicle, AB23A, the FXR antagonist, GS or GS+AB23A. (B) Changes in expression of PPARα, CPT1α, ACADS and LPL in AB23A-treated mice were abrogated by GS. Data are the mean±SD. n=5. $^{*}P$<0.05 *vs* MCD only. $^{\#}P$<0.05 *vs* MCD+AB23A. (C) Representative images of H&E stained liver sections (400×magnification) after GS administration are shown.

Figure 6A illustrates that AB23A induced Apo C-II in a dose-dependent manner, with a maximal change at a dose of 10 μmol/L. Therefore, a dose of 10 μmol/L was chosen for subsequent FXR gene silencing experiments. As shown in Figure 6B, FXR expression was decreased after specific transfection of a siRNA targeting FXR mRNA, as confirmed by Western blot analysis. *In vitro* evidence demonstrated that the changes in Apo C-II, CPT1α, ACADS and LPL induced by AB23A were abrogated by FXR silencing (Figure 6C). These results further demonstrate the involvement of FXR activation in the hepato-protective effects of AB23A.

Discussion

NASH is multifactorial in origin and is considered the hepatic manifestation of metabolic syndrome, which is a major harmful precursor syndrome for numerous diseases[28]. Currently, there is no proven effective therapy for NASH, and liver transplantation is the only option for end-stage NASH. Thus, the development of new drugs for NASH therapy is necessary. In the present study, we demonstrated that AB23A has at least three roles in the protection against MCD-induced NASH. The first role is to decrease hepatic lipogenesis by decreasing hepatic levels of various proteins that are required for triglyceride and fatty acid synthesis and increasing their metabolism by inducing of genes involved in lipid lipolysis and β-oxidation. The second role is to reduce hepatic inflammation by decreasing hepatic inflammatory gene expression. The third role is to reduce liver fibrosis by limiting HSC activation and collagen deposition. Further *in vivo* and *in vitro* studies indicated that the hepato-protective effects of AB23A against NASH were due to FXR-mediated regulation of genes involved in the above processes.

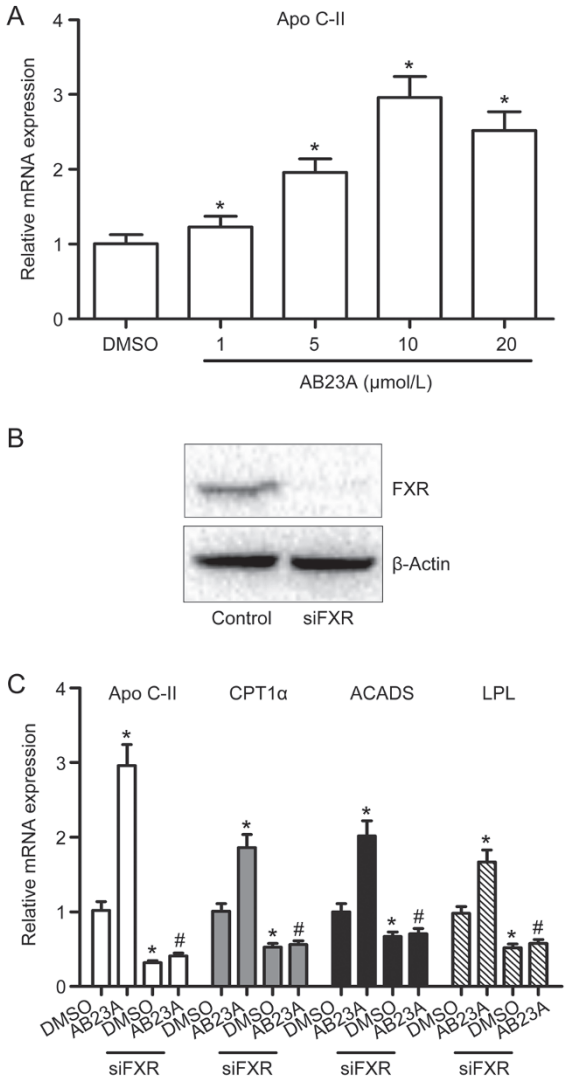

Figure 6. *In vitro* evidence of FXR activation by AB23A. (A) AB23A induced Apo C-II in mouse primary cultured hepatocytes in a dose-dependent manner. Quantitative real-time PCR analysis was performed to measure gene expression and data are expressed as the mean±SD. *n*=5/group. $^{*}P$<0.05 *vs* DMSO vehicle. (B) FXR silencing efficiency was measured by Western blotting. (C) FXR silencing abrogated the regulation of Apo C-II, CPT1α, ACADS and LPL by AB23A in mouse primary hepatocytes. Data are expressed as the mean±SD. *n*=5. $^{*}P$<0.05 *vs* DMSO alone. $^{\#}P$<0.05 *vs* AB23A alone.

There are probably multiple mechanisms leading to NASH, and at least two subsequent hits are required for a healthy liver to develop NASH, cirrhosis and potentially hepatocellular carcinoma. The healthy liver is first sensitized by excessive triglyceride accumulation and is then subsequently exposed to inflammatory and oxidative stress, thus leading to the development of NASH. C57BL/6 mice fed the MCD diet for 4 weeks had significantly increased serum levels of ALT, AST, MCP-1 and mKC and exhibited histological features of NASH, including macrovesicular steatosis, lobular inflammation and pericellular fibrosis (Figure 1). The MCD diet also increased serum triglycerides, free fatty acids and total cholesterol and led to significant hepatic triglyceride accumulation (Figure 2). A variety of genes have been demonstrated to play crucial roles in lipid homeostasis. Hepatic lipogenesis is mainly modulated by SREBP-1c, which is a master regulator of lipid biosynthesis and regulates the expression of other genes involved in triglyceride synthesis, including FAS, ACC1 and SCD1. In this study, SREBP-1c, FAS, ACC1 and SCD1 were all increased by the MCD diet, thus leading to increases in hepatic triglyceride synthesis. AB23A treatment significantly reduced the above protein expressions, thus resulting in decreases in lipid synthesis (Figure 3A). In addition, a decrease in the β-oxidation of fatty acids also leads to MCD-induced accumulation of hepatic lipids. PPARα, a principal regulator of fatty acid oxidation, regulates expression of CPT1α and ACADS, which are two key enzymes in the β-oxidation of fatty acids. AB23A induced PPARα, CPT1α and ACADS expression, resulting in an increase in the β-oxidation of fatty acids (Figure 3B). Furthermore, AB23A treatment induced Apo C-II and inhibited Apo C-III and ANGTPL3 expression, thus leading to LPL activation (Figure 3C). These results suggest that AB23A promotes fatty acid and triglyceride metabolism, thereby resulting in the observed decreases in plasma and hepatic fatty acids and triglycerides. Additionally, increased hepatic mRNA levels of inflammatory markers, including MCP-1 and VCAM-1, and fibrosis markers, including a1(I) collagen, a2(I) collagen, α-SMA, TIMP-1, TGF-β1 and MMP-2 were observed in MCD-fed mice. AB23A treatment significantly lowered the serum levels of the liver enzymes AST and ALT, and the inflammatory chemokines MCP-1 and mKC, while substantially improving hepatic inflammation and fibrosis, as evidenced by the reduction in hepatic lobular inflammation and pericellular fibrosis (Figure 4).

The aforementioned genes involved in lipid homeostasis are regulated by many nuclear receptors, and among them FXR has been proven to be one of the most important upstream nuclear receptors. FXR is the upstream receptor of SREBP-1c, and, through inducing small heterodimer partners (SHPs), FXR suppresses the expression of SREBP-1c[13], thus leading to decreases in the expression of FAS, ACC1 and SCD1. Because we have recently found that AB23A promotes liver regeneration via FXR activation, we hypothesized that AB23A might activate FXR and consequently protect against MCD-induced NASH. We used the FXR antagonist GS in mice to verify this hypothesis. The changes in hepatic gene expression and the amelioration of liver injury in AB23A-treated mice were abrogated by GS administration (Figure 5). The activation of FXR has been demonstrated to be a valuable therapeutic approach for metabolic and inflammatory diseases. Obeticholic acid (OCA, also known as INT-747), a 6a-ethyl derivative of CDCA, is a first-in-class selective FXR agonist, originally described for its anti-cholestatic and potentially broader hepato-protective properties. More recent preclinical studies have shown that OCA increases insulin sensitivity, regulates glucose and lipid metabolism, exerts anti-inflammatory properties, and has marked anti-fibrotic effects[29]. To date, OCA has successfully

completed phase IIb studies for the treatment of NASH[30]. This clinical trial is a double blind, placebo controlled, multicenter study that evaluated treatment with OCA at a dose of 25 mg daily for 72 weeks. The findings indicate that OCA decreases the severity of NASH, as determined by centrally scored liver histology. To further demonstrate whether FXR activation is involved in the hepato-protective effects of AB23A, FXR gene silencing experiments were performed using mouse primary cultured hepatocytes *in vitro*. The results demonstrated that the regulation of Apo C-II, CPT1α, ACADS and LPL by AB23A was abrogated by FXR silencing (Figure 6). Additionally, in a previous study, we have used CDCA, a known FXR agonist, and a luciferase reporter assay in HepG2 cells transiently co-transfected with an FXR expression plasmid and the FXR target gene bile salt export pump (BSEP) promoter reporter vector to demonstrate the effects of AB23A on the transcriptional activation of a FXR target gene[25]. We have found that AB23A activates FXR in a dose-dependent manner and consequently induces BSEP transactivation; this effect was superior to that of an equivalent dose of CDCA.

NASH patients, compared with healthy individuals, have significantly increased serum MCP-1 and IL-8a. mKC is the murine homolog of human IL-8[31]. In the present study, we demonstrated that AB23A treatment reduced hepatic inflammation and decreased liver inflammatory cell infiltration by substantially lowering serum levels of MCP-1, mKC, and the hepatic gene expression of MCP-1 and VCAM-1. Together, these data indicate that through activating FXR, AB23A reduces hepatic levels of SREBP-1c, FAS, ACC1 and SCD1, thereby resulting in decreased hepatic lipogenesis and increases hepatic PPARα, CPT1α, ACADS and LPL expression, and leading to increased lipid metabolism. In addition, AB23A reduces inflammatory cell infiltration via deceasing serum levels of mKC and MCP-1 and the hepatic gene expression of MCP-1 and VCAM-1. The reduction in hepatic fibrosis by AB23A treatment correlates with a reduction in the hepatic gene expression of fibrosis markers.

To observe the hepato-protective effect of AB23A, we selected three doses (15, 30 and 60 mg/kg) administered repeatedly before mouse sacrifice. The dose of 60 mg/kg was the optimal dose of AB23A that demonstrated protection against MCD-induced NASH in mice. This result may support the potential therapeutic use of AB23A. Additionally, 10 mg/kg of GS was the minimal dose that efficiently blocked AB23A-mediated FXR activation in mice.

In summary, AB23A protects against MCD-induced NASH in mice via activating the FXR signaling pathway, thus decreasing the accumulation of lipids in the liver, hepatic lobular inflammation and pericellular fibrosis. Despite a large number of basic science studies searching for novel therapeutic agents to protect against NASH, few options are currently available for clinical use. Our study suggests the possibility that AB23A may be an effective pharmacological agent that protects against NASH.

Acknowledgements

This present study was financially supported by a grant from the National Natural Science Foundation of China (No 81302826, 81473280) and the Program for Key Laboratory of Liaoning Province (No LZ2015027).

Author contribution

Qiang MENG and Ke-xin LIU designed and supervised the experiments and drafted the manuscript. Xing-ping DUAN and Chang-yuan WANG performed the *in vivo* experiments and data analysis. Zhi-hao LIU and Peng-yuan SUN performed the *in vitro* experiments and data analysis. Xiao-Kui HUO, Hui-jun SUN, and Jin-yong PENG helped to analyze data.

References

1 Scorletti E, West AL, Bhatia L, Hoile SP, McCormick KG, Burdge GC, *et al*. Treating liver fat and serum triglyceride levels in NAFLD, effects of PNPLA3 and TM6SF2 genotypes: Results from the WELCOME trial. J Hepatol 2015; 63: 1476–83.
2 Nascimbeni F, Pais R, Bellentani S, Day CP, Ratziu V, Loria P, *et al*. From NAFLD in clinical practice to answers from guidelines. J Hepatol 2013; 59: 859–71.
3 McPherson S, Hardy T, Henderson E, Burt AD, Day CP, Anstee QM. Evidence of NAFLD progression from steatosis to fibrosing-steatohepatitis using paired biopsies: Implications for prognosis and clinical management. J Hepatol 2015; 62: 1148–55.
4 Gan L, Meng ZJ, Xiong RB, Guo JQ, Lu XC, Zheng ZW, *et al*. Green tea polyphenol epigallocatechin-3-gallate ameliorates insulin resistance in non-alcoholic fatty liver disease mice. Acta Pharmacol Sin 2015; 36: 597–605.
5 Ratziu V, Goodman Z, Sanyal A. Current efforts and trends in the treatment of NASH. J Hepatol 2015; 62: S65–S75.
6 Verdam FJ, Dallinga JW, Driessen A, Jonge Cd, Moonen EJC, van Berkel JBN, *et al*. Non-alcoholic steatohepatitis: A non-invasive diagnosis by analysis of exhaled breath. J Hepatol 2013; 58: 543–8.
7 Iyer S, Upadhyay PK, Majumdar SS, Nagarajan P. Animal models correlating immune cells for the development of NAFLD/NASH. J Clin Exp Hepatol 2015; 5: 239–45.
8 Forman BM, Goode E, Chen J, Oro AE, Bradley DJ, Perlmann T, *et al*. Identification of a nuclear receptor that is activated by farnesol metabolites. Cell 1995; 81: 687–93.
9 Zhu Y, Li F, Guo GL. Tissue-specific function of farnesoid X receptor in liver and intestine. Pharmacol Res 2011; 63: 259–65.
10 Cariou B. The farnesoid X receptor (FXR) as a new target in non-alcoholic steatohepatitis. Diabetes Metab 2008; 34: 685–91.
11 Jiao Y, Lu Y, Li XY. Farnesoid X receptor: a master regulator of hepatic triglyceride and glucose homeostasis. Acta Pharmacol Sin 2015; 36: 44–50.
12 Li G, Kong B, Zhu Y, Zhan L, Williams JA, Tawfik O, *et al*. Small heterodimer partner overexpression partially protects against liver tumor development in farnesoid X receptor knockout mice. Toxicol Appl Pharmacol 2013; 272: 299–305.
13 Watanabe M, Houten SM, Wang L, Moschetta A, Mangelsdorf DJ, Heyman RA, *et al*. Bile acids lower triglyceride levels via a pathway involving FXR, SHP, and SREBP-1c. J Clin Invest 2004; 113: 1408–18.
14 Kast HR, Nguyen CM, Sinal CJ, Jones SA, Laffitte BA, Reue K, *et al*. Farnesoid X-activated receptor induces apolipoprotein C-II transcription: a molecular mechanism linking plasma triglyceride

levels to bile acids. Mol Endocrinol 2001; 15: 1720–8.
15 Claudel T, Inoue Y, Barbier O, Duran-Sandoval D, Kosykh V, Fruchart J, *et al*. Farnesoid X receptor agonists suppress hepatic apolipoprotein CIII expression. Gastroenterology 2003; 125: 544–55.
16 Pellicciari R, Fiorucci S, Camaioni E, Clerici C, Costantino G, Maloney PR, *et al*. 6alpha-ethyl-chenodeoxycholic acid (6-ECDCA), a potent and selective FXR agonist endowed with anticholestatic activity. J Med Chem 2002; 45: 3569–72.
17 Gadaleta RM, Cariello M, Sabba C, Moschetta A. Tissue-specific actions of FXR in metabolism and cancer. Biochim Biophys Acta 2015; 1851: 30–9.
18 Wang C, Zhang JX, Shen XL, Wan CK, Tse AK, Fong WF. Reversal of P-glycoprotein-mediated multidrug resistance by Alisol B 23-acetate. Biochem Pharmacol 2004; 68: 843–55.
19 Jin HG, Jin Q, Ryun Kim A, Choi H, Lee JH, Kim YS, *et al*. A new triterpenoid from *Alisma orientale* and their antibacterial effect. Arch Pharm Res 2012; 35: 1919–26.
20 Jiang ZY, Zhang XM, Zhang FX, Liu N, Zhao F, Zhou J, *et al*. A new triterpene and anti-hepatitis B virus active compounds from *Alisma orientalis*. Planta Med 2006; 72: 951–4.
21 Xu YH, Zhao LJ, Li Y. Alisol B acetate induces apoptosis of SGC7901 cells via mitochondrial and phosphatidylinositol 3-kinases/Akt signaling pathways. World J Gastroenterol 2009; 15: 2870–7.
22 Huang YT, Huang DM, Chueh SC, Teng CM, Guh JH. Alisol B acetate, a triterpene from Alismatis rhizoma, induces Bax nuclear translocation and apoptosis in human hormone-resistant prostate cancer PC-3 cells. Cancer Lett 2006; 231: 270–8.
23 Zhang LL, Xu YL, Tang ZH, Xu XH, Chen X, Li T, *et al*. Effects of alisol B 23-acetate on ovarian cancer cells: G_1 phase cell cycle arrest, apoptosis, migration and invasion inhibition. Phytomedicine 2016; 23: 800–9.
24 Hur JM, Choi JW, Park JC. Effects of methanol extract of *Alisma orientale* rhizome and its major component, alisol B 23-acetate, on hepatic drug metabolizing enzymes in rats treated with bromobenzene. Arch Pharm Res 2007; 30: 1543–9.
25 Meng Q, Chen X, Wang C, Liu Q, Sun H, Sun P, *et al*. Alisol B 23-acetate promotes liver regeneration in mice after partial hepatectomy via activating farnesoid X receptor. Biochem Pharmacol 2014; 92: 289–98.
26 Klaunig JE, Goldblatt PJ, Hinton DE, Lipsky MM, Chacko J, Trump BF. Mouse liver cell culture. I. Hepatocyte isolation. In Vitro 1981; 17: 913–25.
27 Anstee QM, Goldin RD. Mouse models in non-alcoholic fatty liver disease and steatohepatitis research. Int J Exp Pathol 2006; 87: 1–16.
28 Filozof C, Goldstein BJ, Williams RN, Sanyal A. Non-alcoholic steatohepatitis: limited available treatment options but promising drugs in development and recent progress towards a regulatory approval pathway. Drugs 2015; 75: 1373–92.
29 Mudaliar S, Henry RR, Sanyal AJ, Morrow L, Marschall HU, Kipnes M, *et al*. Efficacy and safety of the farnesoid X receptor agonist obeticholic acid in patients with type 2 diabetes and nonalcoholic fatty liver disease. Gastroenterology 2013; 145: 574–582.e571.
30 Neuschwander-Tetri BA, Loomba R, Sanyal AJ, Lavine JE, Van Natta ML, Abdelmalek MF, *et al*. Farnesoid X nuclear receptor ligand obeticholic acid for non-cirrhotic, non-alcoholic steatohepatitis (FLINT): a multicentre, randomised, placebo-controlled trial. Lancet 2015; 385: 956–65.
31 Zhang S, Wang J, Liu Q, Harnish DC. Farnesoid X receptor agonist WAY-362450 attenuates liver inflammation and fibrosis in murine model of non-alcoholic steatohepatitis. J Hepatol 2009; 51: 380–8.